Taylor & Francis
Taylor & Francis Group

Large "Pillow" Fullerenes Hydrogenated at the Inter-sheet "Seam"

Alexandru T. Balaban and Douglas J. Klein

MARS, Texas A&M University at Galveston, Galveston, Texas, USA

Ovidiu Ivanciuc

HBC & G, University of Texas Medical Branch, Galveston, Texas, USA

Abstract: In a previous paper on large "pillow" fullerenes, various systems were described with 12 pentagons connecting 2 parallel hexagonal arrays of benzenoid rings (graphene fragments functioning as the faces of the "pillow") on top of each other. Additional bonds between these identical arrays formed only from sp^2-hybridized carbon atoms gave rise to hexagons and 12 pentagons along the "seam" or "rim." High steric strain was associated with curvature around the pentagons due to connections between the 2 pillow faces involving bonds between 2 sp^2-hybridized carbon atoms. The present paper examines similar "quasi-graphitic" structures in which some carbon atoms of the rim between the two raphene faces have hydrogen atoms attached to them, i.e., have sp^3-hybridization, alleviating thereby some strain.

Keywords: Partly hydrogenated fullerenes, "pillow" fullerenes, flattened carbon cages

INTRODUCTION

In a previous paper (1) published in this journal we presented calculations on the possibility of connecting the margins of two large graphene sheets resulting in flat cages of elemental carbon. The idea was to explore the possibility of a type of graphite without dangling bonds or heteroatoms at the margins of the graphene sheets.

   Address correspondence to Professor Alexandru T. Balaban, MARS, Texas A&M University at Galveston, Galveston, TX 77553-1675, USA. E-mail: balabana@tamug.edu

The two parallel graphene sheets then give rise to a "pillowcase fullerene" with 12 pentagons and a large number of hexagons (so that we called such a structure a "pill-fullerene" or "pillowene" for brevity). These structures resemble in shape, in the ideal case, a healthy red-blood cell (erythrocyte). This structure should develop intramolecular attractive interactions between the central portions of the 2 graphene sheets that in graphite are at a distance of about 330 pm (but with larger distances at the "seams" of our pillow fullerenes because of the strain caused by bonds involving pairs of sp^2-hybridized carbon atoms). An additional factor to be considered for the central portions is the manner in which the carbon atoms of the 2 quasi-planar graphene sheets are placed on top of each other: more favorable (attractive) interactions occur when carbon atoms of one sheet are placed over center regions of hexagons of the other sheet, as in (multilayer) graphite. Even if this ideal geometry cannot be attained, pillow fullerenes with a biconvex lens-shaped geometry would have smaller voids within the carbon cages, and better packing in the condensed state.

Bonds in fullerene carbon cages give rise to strain when bond angles differ from $120°$ as in 5-membered rings, or when other factors cause the 3 sp^2-bonds of a carbon atom to become pyramidalized, as happens at the "seams" (rims) of the pillow-fullerenes.

In the present paper we present results of an investigation of what happens when one seeks to alleviate the strain at the "seams" of such "pillow" carbon cages if some carbon atoms at the margins of the graphene sheets also have hydrogen atoms. Placement of the hydrogen atoms on more pyramidalized carbon atoms then promotes sp^3-hybridization at these sites, which appear as trigonal corners on a polyhedron, with 1 bond external (to a hydrogen atom), and thereby lead to a plausible associated reduction in (angle) strain. If the sp^3-hybridized carbon atoms adopt their ideal angles of $\approx 109.5°$, then each atom gives a net Cartesian angle defect $\mathbf{s} \approx 360° - 3 \times 109.5° = +31.5°$, which further is the net Gaussian curvature at the corner. Therefore approximately 23 of these atoms would accommodate all the Gaussian curvature of $720°$ ($=4\pi$ radians) required of closed surfaces homeomorphic to a sphere. But especially with anisotropic curvature (as with large pillow fullerenes), somewhat smaller numbers of sp^3-hybridized carbon atoms may be appropriate, essentially because the rings around the girth are not planar. To understand this point, let us consider a hexagonal ring with a bending only in the direction orthogonal to the dashed line in Figure 1a, i.e., the crease of folding is along the direction of this dashed line. Then the hexagon may be imagined to be broken up into 2 triangles and a square as in Figure 1b, with each of these smaller polygons more nearly planar. Though there are no bonds along the dotted lines in Figure 1b, the Gauss theorem (for the net Gaussian curvature) relates more neatly to the associated surface composed from planar polygons. Each sum $\mathbf{s}$ of the resultant 4 angles at each of the 4 atoms

(a) **(b)**
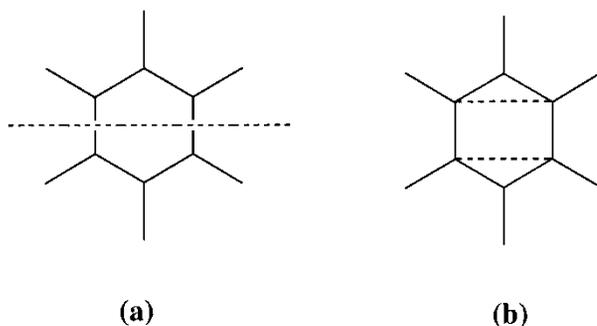
Figure 1. Two different kinds of Gaussian curvature: (a) hexagons bent once along a median line; (b) hexagons bent twice.

incident to the dashed lines should be larger than the sums of the three bond angles, so that the actual Gaussian curvature associated to each vertex is greater than what we identify from the use of bond angles, and as a consequence a lesser number of sp^3-hybridized carbon atoms may be favorably so accommodated.

In the present context, an obvious way to achieve this alleviation of steric strain would be to have partial hydrogenation along the rim of the pillow fullerene. The present paper explores systematically these possibilities, examining the same systems formed by two hexagonal graphene arrays connected along the rim by 12 pentagons, but having in addition some sp^3-hybridization of carbon atoms at the rim between the 2 graphene faces. The resulting structure would no longer be a proper fullerene, but a *partly hydrogenated pillow fullerene*, and again, with increasing size of the graphene fragments, the relative amount of hydrogen becomes negligibly small. Indeed natural graphite certainly ordinarily contains non-carbon atoms at the boundary to accommodate what would otherwise be dangling bonds. In particular, it is recognized that for impure coals and graphitic carbons, there is always a measurable quantity of hydrogen (2, 3).

Indeed, with the hydrogen atoms confined to the region of the rim between the 2 joined graphene sheets, the present valence-saturated structures are more nearly elemental carbon than natural graphite, the more so as the dimension of the pillow-fullerene increases. Another candidate for more purely graphitic structures is obtained by the realization of the theoreticians' "cyclic boundary conditions," whence edges, rims, non-hexagonal rings, and dangling bonds all may be eliminated to yield what have been termed "elemental benzenoids," or "bucky-tori" or "crop circles," but these are not further considered here.

The discovery of fullerenes, honored by the award of the Nobel Prize for Chemistry (4–6), was soon followed by the formulation of the "isolated

pentagon rule" (7, 8) stating that all stable fullerenes starting with C_{60} and C_{70} have no contiguous pentagons. Experimentally it was discovered that occasionally the dangling bonds at the rim of graphene sheets are avoided by bending and pleating these sheets (9, 10). Scott and coworkers (11) recently succeeded in synthesizing buckminsterfullerene C_{60} by assembling together in a rational synthesis the 20 benzenoid rings and 12 pentagons in a hydrogenated compound $C_{60}H_{30}$, and dehydrogenating it. The literature on hydrogenated fullerenes has recently been reviewed (12). It was shown by Fowler and coworkers (13) that the most stable hydrogenated C_{24} fullerene has 12 hydrogen atoms along an equatorial circumference. The idea of relieving the curvature strain of tetrahedral-symmetry fullerenes by adding a hydrogen atom at each corner was published in reference (14). The general interrelation between geometric curvatures and stresses is reviewed in reference (15).

PILLOW FULLERENES HYDROGENATED AT THE
INTER-SHEET "SEAM" OR "RIM"

As in the preceding paper (1), we simplify our molecular mechanics optimizations by starting from 2 hexagonal "super-coronenic" graphene sheets. There are 2 possibilities of defining such a hexagonal graphene sheet: its edges can be either (i) zigzag lines as in long acene benzenoids having a linear dualist graph, or (ii) "armchair" edges as in long fibonacenes with a zigzag dualist graph (16). The six "corners" of the graphene sheet in the former case are represented by a single benzenoid ring (a in Figure 2) and in the latter case either by a single benzenoid ring or by a naphthalenic pair of rings (Figure 2b and 2c respectively). In the present paper we will not consider armchair systems.

   With the former type (i) of sheet edges, in the simplest case, we replace the pairs of sp^2-hybridized carbon atoms at the "corners" of the hexagonal cuts by pairs of sp^3-hybridized carbon atoms, so that when the inter-sheet bonds are formed, there will be 12 such bonds for each sheet emerging from 12 sp^3-hybridized carbon atoms. The facing sheet may be rotated with various angles relative to the facing parallel graphene sheet so as to avoid forming any 4-membered rings, and we will analyze the resulting possibilities of the resulting partly hydrogenated "pillow" carbon cages C_nH_{24}. If 6 4-membered rings were allowed instead of 12 5-membered rings, the central portions of the graphene sheets would have carbon atoms exactly superimposed (in axial projection) on each other, leading to unfavorable interactions between the sheets (discussed later).

   A peri-condensed polyhex or benzenoid hydrocarbon with a hexagonal symmetry (super-coronoid) having k hexagons on each external edge of the

(a)

(b)   **(c)**
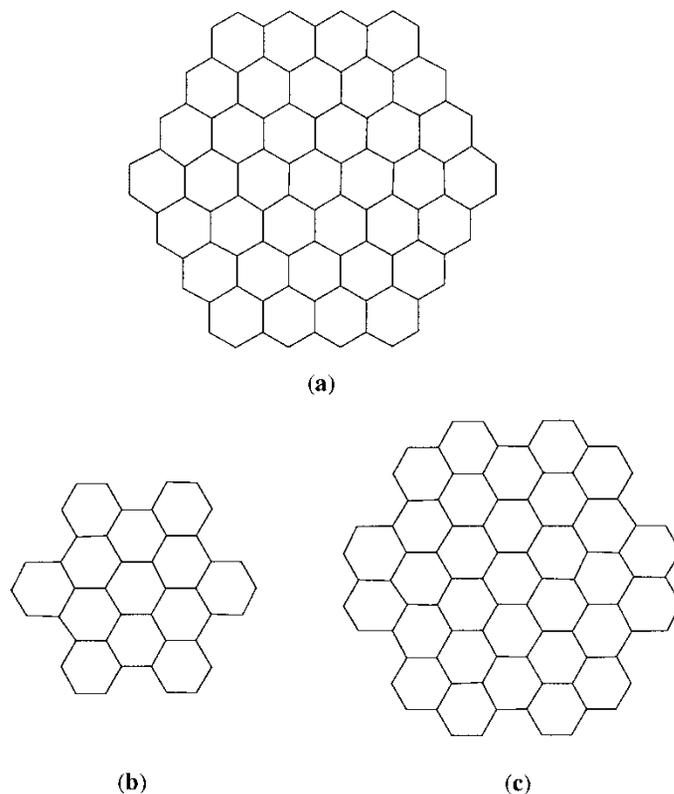
Figure 2. (a) A zigzag hexagonal graphene sheet with k = 4; (b) and (c) armchair hexagonal graphene sheets with a benzenoid subgraph or a naphthalene subgraph at the corners, respectively.

graphene hexagonal cut has a total of $n = 6k^2$ carbon atoms and $3k(k-1)+1$ benzenoid rings. There are 6k dangling bonds around the edge of this hexagonal cut and these will have to become inter-plane bonds, forming 6k additional rings along the seam. In pillow fullerenes all these bonds along the seam are sp^2–sp^2 bonds causing considerable strain.

Although we are motivated by the possibility of large quasi-graphitic systems, calculations can be conveniently made only for the smaller systems with $k \leq 6$, but they will allow us to extrapolate the results to the large systems. All such systems have exactly 12 pentagons along the inter-sheet "seam."

Similarly to previous notation, the 6k dangling sigma bonds around the circumcoronene will be numbered cyclically starting from the dangling bond that is closest to a "corner" of one edge. Dangling bonds of 2

circumcoronenes lying parallel on top of each other will annihilate each other such that bond i at the edge of one array becomes connected to dangling bond $i + p$ at the edge of the other circumcoronene, and the process continues cyclically for i ranging from 1 to 6k. In other words, the two identical parallel arrays are rotated (or off-set) with respect to each other by the fraction $p/6k$ of a full rotation. If $p = 0$, then the rotation is nil, so that the resulting faces at the rim connecting the two circumcoronenes would consist of six squares and $6(k - 1)$ hexagons. We have seen that this situation introduces angle strain, and does not lead to favorable inter-sheet interactions, with carbons in the two sheets sitting directly over one another. For any $p > 0$ and $p < k$, the resulting new faces along the rim will be 12 pentagons and $6(k - 2)$ hexagons. We shall concentrate on this last type of system, and examine the possible ways to alleviate the strain by adding hydrogen atoms to some carbons such that the resulting structure remains Kekuléan (in the sense that it accommodates a nearest neighbor-paired Kekulé structure). The smaller p values lead to pillowenes with more pronounced, sharper delineated "corners" of the hexagonal pillow.

When the corner benzenoid rings have their pair of carbon atoms to which a pair of hydrogen atoms is added, these carbon atoms would adopt sp^3-hybridization, and some of the 6k inter-plane bonds in the pillow carbon cage formed in the subsequent "dehydrogenating dimerization" would become sp^2–sp^3 or sp^3–sp^3 inter-sheet bonds. In turn, this alleviates appreciably the bond strain and allows the graphene sheets to stay approximately parallel so as to make possible intramolecular van der Waals interactions between the two graphene sheets, leading to the erythrocyte shape of the partly hydrogenated carbon cage. By contrast, sp^2–sp^2 inter-sheet bonds lead to high strain and, for smaller n values, to a pronounced convex shape as in a magnifying lens. All pillow fullerenes described in the present paper have a biconvex lens-shape.

For large k values the corresponding systems will have numerous sp^2–sp^2 inter-sheet bonds (in addition to the 24 or less sp^2–sp^3 or sp^3–sp^3 inter-sheet bonds). However, for $\sim$k carbons on the zigzag edge of a hexagonal graphene sheet, the edge strain will be proportional to $\sim k \sim \sqrt{n}$, while the number of nearby attractive van der Waals interactions will be $\sim n$. Therefore with increasing n, the van der Waals attractive forces between the 2 faces of the pillow fullerene will overcome the bulging from strain at the rims and favor a collapsed erythrocyte-shape over a biconvex lens-shape, as will be discussed in more detail shortly.

Figures illustrating the present paper have been produced by minimizing energies with the semiempirical AM1 method as given in the Hyperchem program, and the results are indicated in Table 1. The stereo-views are drawn with the help of the CambridgeSoft (CS) Chem3D Pro software (version 3.2) within the CS ChemOffice program.

Table 1. Characteristics of the partly hydrogenated pillow fullerenes

| ID	Formula	k	p	Number of hexagons	Number of sp^2 atoms	Number of inter-sheet bonds			
						sp^3-sp^3	sp^2-sp^3	sp^3-sp^3	Total
1	$C_{48}H_{24}$	2	1	14	24	12	0	0	12
2	$C_{108}H_{24}$	3	1	44	84	6	12	0	18
3	$C_{192}H_{24}$	4	2	86	168	24	0	0	24
4	$C_{192}H_{24}$	4	1	86	168	6	12	6	24
5	$C_{300}H_{24}$	5	2	140	276	0	24	6	30
6	$C_{300}H_{24}$	5	1	140	276	12	12	6	30
7	$C_{432}H_{24}$	6	3	216	408	0	24	12	36
8	$C_{432}H_{24}$	6	2	216	408	0	24	12	36
9	$C_{432}H_{24}$	6	1	216	408	6	12	18	36

PILLOW PARTLY-HYDROGENATED CARBON CAGES ("PILLOWENES") C_nH_{24}

All the following rim-partly-hydrogenated carbon cages C_nH_{24} have 12 pentagonal rings and 24 sp^3-hybridized carbon atoms, and therefore their total number of sp^3–sp^3 and sp^3–sp^2 "inter-plane" bonds cannot be higher than 24. The numbers of hexagonal rings, of sp^2-hybridized carbon atoms and of the three kinds of "inter-plane" bonds are presented in Table 1. We consider various hexagonally-symmetric super-coronenes with several k values ranging from coronene with k = 2 up to super coronenes with k = 6, which leads to partly-hydrogenated pillow fullerenes (by pairwise association followed by hydrogenation of inter-sheet C—C bonds in pentagonal rings):

1. Coronene, k = 2, gives rise to a single off-set p = 1 and associated cage $C_{48}H_{24}$ (**1**) having 14 hexagonal rings in addition to the 12 pentagons, 24 carbon atoms with sp^2 hybridization, and 12 sp^3–sp^3 inter-sheet bonds. This cage is depicted in Figure 3.
2. Circum-coronene, k = 3, gives rise to a single off-set p = 1 and associated cage $C_{108}H_{24}$ (**2**) having (in addition to the 12 pentagons) 44 hexagonal rings, 84 carbons with sp^2 hybridization, 6 sp^3–sp^3 and 12 sp^2–sp^3 inter-sheet bonds. A Schlegel diagram is presented in Figure 4, and stereo-views of the lens-shaped pillow fullerene are shown in Figure 5 (face and profile). It may be seen that the 24 CH groups (indicated by black dots in Figure 4) of the 12 cyclopentene rings isolate 2 sets of almost
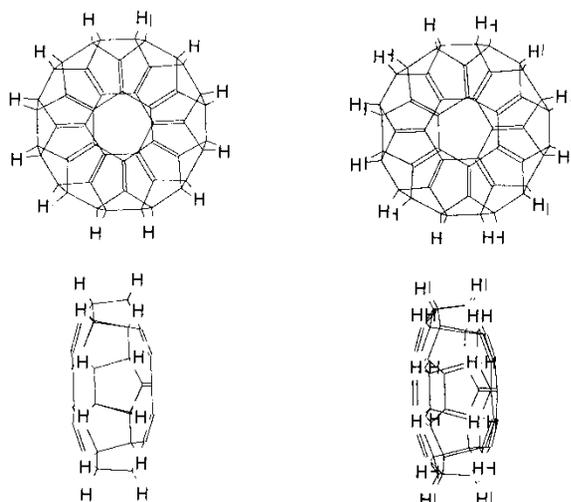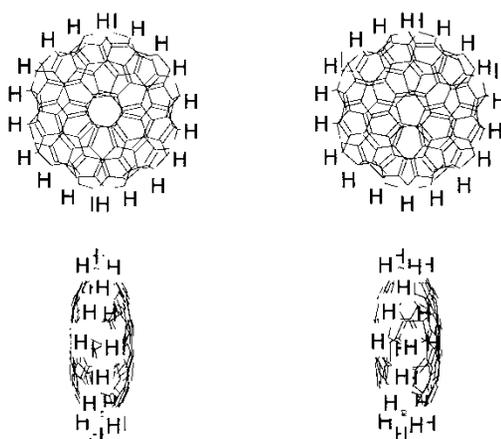

Figure 3.   Stereoviews of the hydrogenated pillow fullerene **1**, $C_{48}H_{24}$ with k = 2.
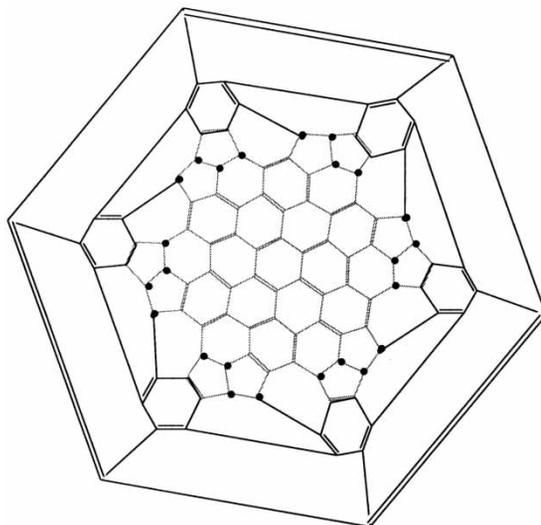
Figure 4. A Schlegel diagram of the hydrogenated pillow fullerene **2**, $C_{108}H_{24}$ with k = 3. The dots denote CH groups.

planar pericondensed 6-membered rings in the fully aromatic hexabenzo[*b-c,ef,hi,kl,no,qr*]coronenes, each with 42 carbon atoms. For better visualization, the inner set has thinner edges than the outer set. In addition, 6 thicker edges connect the outer set to a marginal CH group of the 6 (CH)$_4$ chains. As one may further observe from Figure 4, the C—C single bonds of the 6 (CH)$_4$ chains separating the 2 pericondensed benzenoids are part of
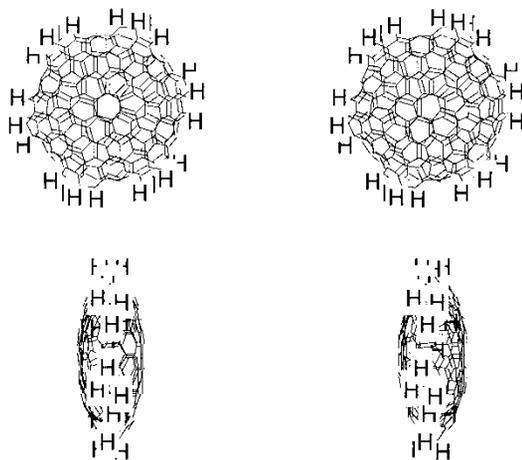

Figure 5. Stereoviews of the hydrogenated pillow fullerene **2**, $C_{108}H_{24}$ with k = 3.

the 6 pairs of pentagons sharing an edge, of 12 1,3-hexadienic rings, and of 6 1,4-hexadienic rings.

3. The next super-coronene with $k = 4$ corresponds to cages $C_{192}H_{24}$ with 86 hexagonal rings in addition to the 12 pentagons, involving 24 carbons with sp^3 hybridization and 168 carbons with sp^2 hybridization. Now one has not 1 but 2 possible off-sets ($p = 1$ and 2) for interconnecting the 2 parallel graphene cuts. The "isolated pentagon rule" for stable fullerenes (4, 5) is no longer relevant for the present cage systems in which the pentagons contain sp^3-hybridized carbon atoms. One of these 2 possibilities yields a cage (**3**) with 24 sp^3–sp^3 "inter-plane" bonds and no adjacent pentagons (Figure 6). The rotation between the 2 parallel graphene sheets corresponds to $p = 2$, and the shape of the "pillow" is almost round. The other possibility corresponding to a rotation with $p = 1$ and yielding a more hexagonal-shaped "pillow," is a cage (**4**) with 6 sp^3–sp^3, 12 sp^2–sp^3 and 6 sp^2–sp^2 inter-sheet bonds, which does contain adjacent pentagons (Figure 7).

4. The next super-coronene with $k = 5$ corresponds to cages $C_{300}H_{24}$ with 140 hexagonal rings in addition to the 12 pentagons, involving 24 carbons with sp^3-hybridization and 276 carbons with sp^2 hybridization. Again one has 2 possible off-sets for interconnecting the 2 parallel graphene cuts. One of these yields with $p = 2$ a cage (**5**) with 24 sp^2–sp^3 and 6 sp^2–sp^2 inter-sheet bonds with no adjacent pentagons (Figure 8); the other with $p = 1$ affords a cage (**6**) with 12 sp^3–sp^3, 12 sp^2–sp^3, and 6 sp^2–sp^2 inter-sheet bonds, and contains adjacent pentagons (Figure 9).
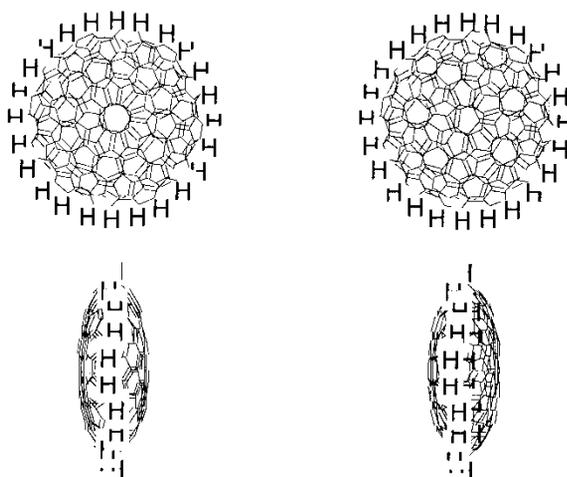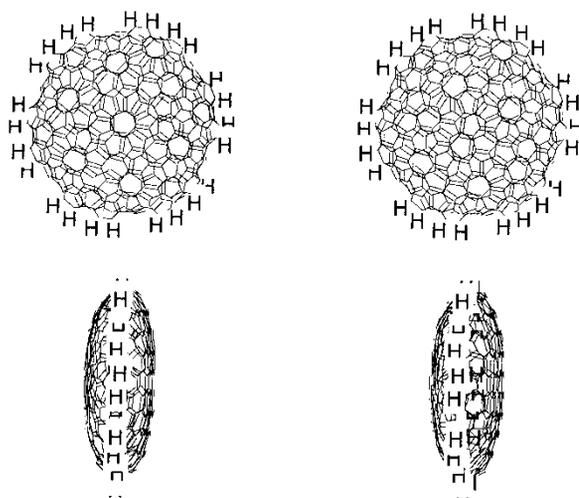

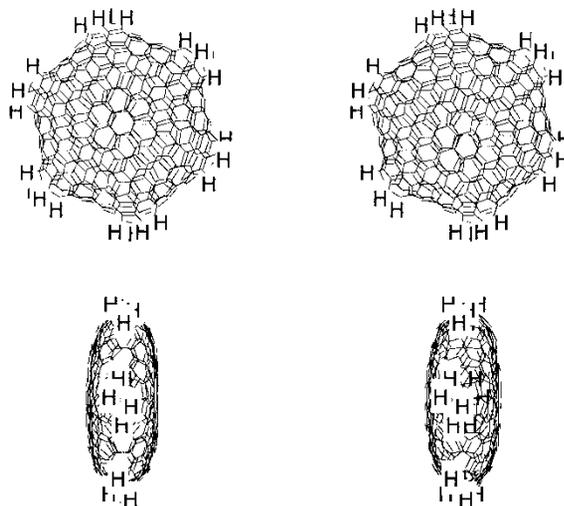**Figure 6.** Stereoviews of the hydrogenated pillow fullerene **3**, $C_{192}H_{24}$ with $k = 4$ and $p = 2$.

Figure 7. Stereoviews of the hydrogenated pillow fullerene **4**, $C_{192}H_{24}$ with k = 4 and p = 1.

From this case onwards with increasing k values, when there are to be just 24 hydrogen atoms, one cannot avoid the presence of sp^2-sp^2 inter-sheet bonds, which will cause higher steric strain than the other two bond types.
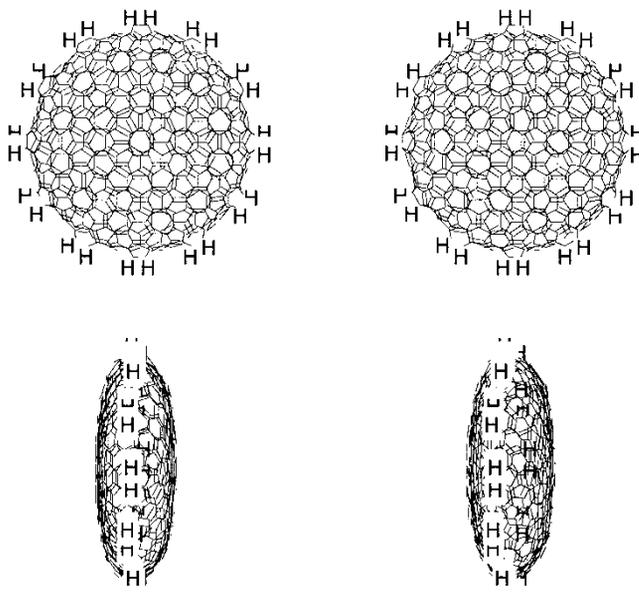

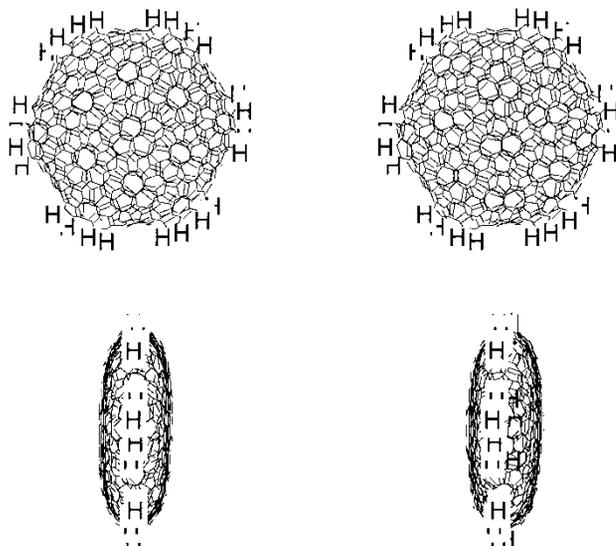**Figure 8.** Stereoviews of the hydrogenated pillow fullerene **5**, $C_{300}H_{24}$ with k = 5 and p = 2.

Figure 9. Stereoviews of the hydrogenated pillow fullerene **6**, $C_{300}H_{24}$ with $k = 5$ and $p = 1$.

5. Finally, the super-coronene with $k = 6$ affords (by hydrogenating dimerization) $C_{432}H_{24}$ cages with 146 hexagonal rings in addition to the 12 pentagons, involving 24 carbons with sp^3-hybridization and 408 carbons with sp^2-hybridization. Now one has 3 possibilities of connecting the 2 parallel graphene sheets. The first one (**7**) with $p = 3$ has 24 sp^2–sp^3 and 12 sp^2–sp^2 inter-sheet bonds apart from each other, and has a round shape, since the pentagons are isolated and equidistant from each other (Figure 10). The next one (**8**) with $p = 2$ also has 24 sp^2–sp^3 and 12 sp^2–sp^3 inter-sheet bonds, but they are adjacent to each other; cage (**8**) has a less round shape, as the pentagons are non-adjacent but not equidistant (Figure 11). The third cage (9) with $p = 1$ has 6 sp^3–sp^3, 12 sp^2–sp^3, and 18 sp^2–sp^2 inter-sheet bonds, and has a hexagonal shape with the "corners" formed by pairs of adjacent pentagons (Figure 12).

In Table 2 we present the results of quantum-chemical calculations (AM1) for all these pillow carbon cages partly-hydrogenated at the pentagons on the rim. The total energy is composed from the "isolated atomic energy" that is the same for isomeric systems, and the "binding energy" that differs among isomers. The sixth column of Table 2 contains heats of formation. The upper part of the Table 2 presents global values, and for making comparisons among cages with different numbers of carbon atoms the lower part of Table 2 presents normalized values per carbon atom. As expected, standard heats of formation per carbon atom are highest and the total and binding

Figure 10. Stereoviews of the hydrogenated pillow fullerene **7**, $C_{432}H_{24}$ with k = 6 and p = 3.

Figure 11. Stereoviews of the hydrogenated pillow fullerene **8**, $C_{432}H_{24}$ with k = 6 and p = 2.
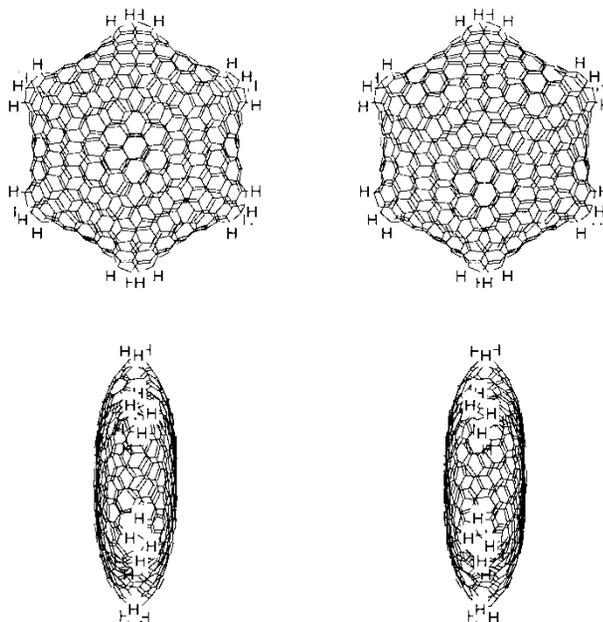
Figure 12. Stereoviews of the hydrogenated pillow fullerene **9**, $C_{432}H_{24}$ with k = 6 and p = 1.

energies are lowest for the smaller cages partly-hydrogenated at the pentagons on the rim. An unexpected affect appears on comparing isomeric cages: for systems with k = 4 or 5 the isomers with non-adjacent hydrogenated pentagons have higher heats of formation than systems with adjacent pentagons, whereas the opposite is true for the 3 systems with k = 6. At k = 6, the further away from each other are the partly hydrogenated pentagons at the rim, the more positive the heats of formation.

Some further comment is warranted as concerns non-bonding interactions and their role in determining stability-favored off-sets and global shape of the cages. The non-bonding interactions between 2 carbon atoms in the 2 graphene layers can plausibly be imagined to entail 2 contributions: first, a directional multipolar interaction between the two carbons; and second, a non-directional dispersion interaction. For the first of these interactions, each sp^2-hybridized carbon is naturally viewable as a small quadrupole with its axis oriented normal to the local molecular plane, whence with 2 carbons from different layers set directly over one another, a quadrupole-quadrupole repulsion results. For two carbons from different layers not placed over one another the repulsion should diminish, and at sufficient angles for the interatomic axis from the normal, the interaction should become

Table 2. Quantum-chemical results (AM1) for partly hydrogenated pillow fullerenes

ID	Formula	Total energy (kcal/mol)	Isolated atomic energy (kcal/mol)	Binding energy (kcal/mol)	Heat of formation (kcal/mol)	HOMO-LUMO gap (eV)
1	$C_{48}H_{24}$	−149,086	−139,975	−9,111	342	7.5182
2	$C_{108}H_{24}$	−325,634	−306,708	−18,926	781	6.1355
3	$C_{192}H_{24}$	−572,949	−540,133	−32,816	1,246	5.2368
4	$C_{192}H_{24}$	−572,897	−540,133	−32,764	1,297	4.9436
5	$C_{300}H_{24}$	−890,971	−840,252	−50,720	1,798	4.3735
6	$C_{300}H_{24}$	−890,925	−840,252	−50,673	1,844	3.6102
7	$C_{432}H_{24}$	−1,279,771	−1,207,063	−72,708	2,367	4.1151
8	$C_{432}H_{24}$	−1,279,808	−1,207,063	−72,745	2,330	4.0007
9	$C_{432}H_{24}$	−1,279,848	−1,207,063	−72,785	2,290	4.1521
Divided by the number of carbon atoms						
1	$C_{48}H_{24}$	−3,105.96	−2,916	−189.81	7.125	
2	$C_{108}H_{24}$	−3,015.13	−2,840	−175.24	7.231	
3	$C_{192}H_{24}$	−2,984.11	−2,813	−170.92	6.490	
4	$C_{192}H_{24}$	−2,983.84	−2,813	−170.65	6.755	
5	$C_{300}H_{24}$	−2,969.90	−2,801	−169.07	5.993	
6	$C_{300}H_{24}$	−2,969.75	−2,801	−168.91	6.147	
7	$C_{432}H_{24}$	−2,962.43	−2,794	−168.31	5.479	
8	$C_{432}H_{24}$	−2,962.52	−2,794	−168.39	5.394	
9	$C_{432}H_{24}$	−2962.61	−2,794	−168.48	5.301	

attractive (though of a lesser strength because of the associated greater distance). For the dispersion interaction the result between 2 planes should always be attractive, and the more so the closer the 2 planes. Thence as a result of these 2 interactions one should imagine that: first, a favoring of larger off-set p ($\approx$k/2); and second, a tendency at least at suitable larger off-set to bring the 2 graphene sheets to a separation comparable to that in ordinary graphite.

A further question concerns the influence of the stress at the edges of the inter-linked graphene sheets, this favoring less bending and hence more pillow-shaped structures. Thence a comparison of these 2 tendencies is appropriate, in which case we consider a pillow-fullerene with n carbon atoms. With a consequent number of edge atoms $\sim\sqrt{n}$, there evidently is a curvature strain energy $\sim\sqrt{n}$, whereas the net non-bonding energy interaction should be $\sim$n. The proportionality for the curvature stress should be larger than for the non-bonding attraction, and the signs are such as to favor opposite influences in so far as the separation between layers goes. Thus at small n one may expect a sizable separation between the 2 graphene layers, at larger n (i.e., at larger k) one may expect that the 2 layers close down to a separation comparable to that of graphite. In conclusion, we expect that for sufficiently large k, the healthy (near flat) erythrocyte shape is favored, especially the more so for the higher off-set (higher p value), which should be favored over the corresponding lower off-set structures.

Finally these expectations may be compared with our current quantum-chemical semiempirical results displayed in Table 2. In agreement with our expectations for smaller k, the favored geometries appear like a pronouncedly biconvex lens, which becomes slimmer as k increases from 3 to 6, but the flatness is not yet seen even at k = 6, which is thus not sufficiently large. First, one may note that attractive dispersion interactions are a correlated-electron effect typically absent from SCF computations, in which class the AM1 computations fall (though AM1 is atypical from an ab initio view in being highly parameterized, sometimes against experimental data). Second, our qualitative expectations suggest that larger off-set p is favored, which is indeed observed for k = 4 and 5, but reversed at k = 6. The larger off-set-favoring quadrupole-quadrupole effect is probably adequately handled in SCF computations, so that the computed result at k = 6 would only be rationalized through some sort of difference of curvature effects at the boundary. We still anticipate a favoring of larger off-set p at larger k.

On looking at the HOMO-LUMO gap in the upper part of Table 2, one sees that this gap decreases (presumably ultimately to zero as in graphite (17) with increasing n (or k), approximately proportionally to $1\sqrt{n}$, but the gap is still high even for n = 6. For the same n or k values (k = 4 and k = 5), the HOMO-LUMO gap is larger for larger off-set values p, but for k = 6 again we find no clear monotonic variation with p.

## FURTHER PARTLY-HYDROGENATED PILLOWENES C_nH_{36} AND C_nH_{48}

Less strained types of lens-shaped (or, ideally, erythrocyte-shaped) carbon cages may be possible with more hydrogen atoms at the "seams" between the 2-graphene sheets, thereby reducing or canceling the number of sp^2-sp^2 inter-sheet bonds. With 36 hydrogen atoms symmetrically arranged around the periphery, one obtains quinonoid structures (Fig. 13) which, being less stable, are not discussed further ($C_{60}H_{36}$ is not stable in air, but can be studied in the absence of oxygen (18)). However, with 48 hydrogen atoms it is possible to have partly hydrogenated "pillow-fullerenes" with aromatic pericondensed "faces" that are less strained than the systems with 24 hydrogen atoms that were discussed in the preceding section for several k values. One such case (Figure 14) is that of the cage with k = 5, $C_{300}H_{48}$, which is also not discussed here in detail. With even more hydrogen atoms added to 5- and 6-membered rings on the rim, it would be possible to avoid completely sp^2-sp^2 inter-sheet bonds, but again such hydrogen-rich systems are not here discussed in more detail.

CONCERNING THE POSSIBILITY OF VERIFYING EXPERIMENTALLY THE THEORETICAL PREDICTIONS

The theoretical pillow fullerenes envisaged here should have reduced void spaces in the interior of the carbon cages, so as to have lentil-shaped
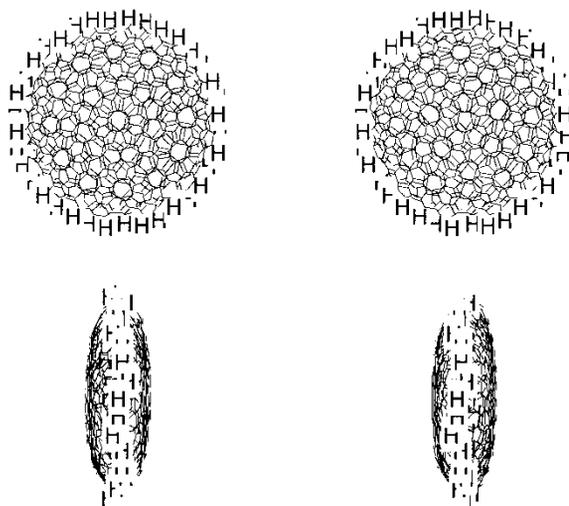
Figure 13. Stereoviews of the hydrogenated pillow fullerene $C_{432}H_{36}$.
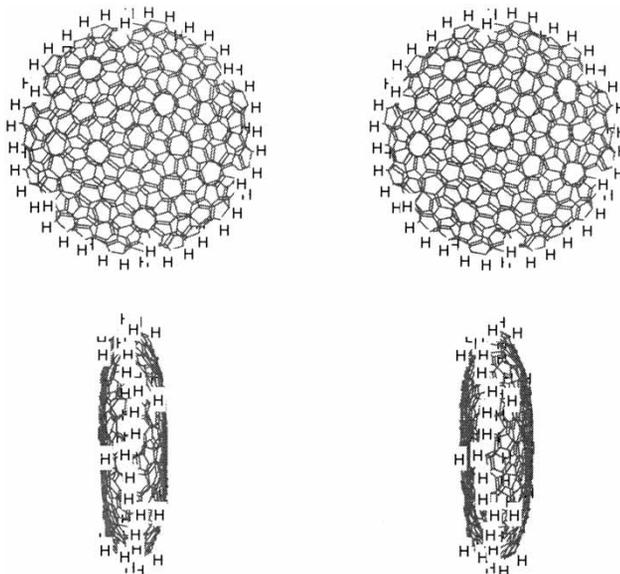
Figure 14.

geometries. Therefore the packing in solid phase would be tighter. The ideally envisaged erythrocyte shapes with 2 parallel flat graphene sheets at a comparable distance as in graphite should eventually be attainable at rather large k values, though with further hydrogenation this theoretical "cross-over" k value should diminish.

It would, however, be interesting to speculate that incipient hydrogenation of large fullerenes under extremely high pressure (possibly in a diamond anvil) could result in reducing preferentially some pentagons along the rim of pillow-shaped fullerenes. As it is well known, stable fullerenes obey the "isolated pentagon rule" so that the smallest such fullerene with all 12 pentagons arranged on an "equatorial belt" would have almost 200 carbon atoms. Therefore any such experiment would have to use a smaller fullerene and to aim at a slightly flattened carbon cage formed by hydrogenating only a few pentagons arranged on an "equatorial belt." The reaction would have to be tried in concentrated solution using a good solvent (for instance a methyl- or a chloro-naphthalene) and a compound that generates diimine thermally or photochemically, or hydrogen plus a homogeneous Wilkinson-type hydrogenation catalyst.

In the literature there are many examples of hydrogenated or halogenated fullerenes formed by preferential addition to double bonds shared by a pentagon and a hexagon, rather than the bonds shared by 2 hexagons; equatorial belts of sp^3-hybridized carbon atoms are often observed, or computed to be

the most stable. As a result, the addition product is a "squashed fullerene" rather than a "pillow fullerene" because it is derived from fullerenes that do not have 2 graphene sheets connected by pentagons distributed on an equatorial belt (19–34).

CONCLUSIONS

On adding 24 hydrogen atoms to double bonds of the 12 pentagons arranged on an equatorial belt of the pillow fullerenes described in an earlier paper (1), the steric strain is diminished. The sphericity is reduced, but at the sizes presently considered, the shape of the resultant pillow fullerene partly hydrogenated at the inter-sheet "seam" remains similar to a biconvex lens, at least at the sizes (up to $C_{432}H_{24}$) treated here. These structures, and especially larger presumably flattened erythrocyte-shaped partly hydrogenated pillowenes, provide a novel type of structure, more "graphitic" than ordinary natural graphites.

ACKNOWLEDGMENT

REFERENCES

1. Balaban, A.T., Klein, D.J., and Seitz, W.A. (2000) Large "pillow" fullerenes as graphite without dangling bonds. *Fuller. Sci. Technol.*, 8: 249–265.
2. Gerstein, B.C., Murphy, P.B., and Ryan, L.M. (1982) *Coal Structure*; Meyer, R.A., Ed.; Academic Press: New York, 87–129.
3. Michel, D., Pruski, M., and Gerstein, B.C. (1994) NMR of petroleum cokes. Parts I and II. *Carbon*, 32 (31–40): 41–49.
4. Curl, R.F. (1997) Dawn of the fullerenes: experiment and conjecture. *Rev. Mod. Phys.*, 69: 691–702.
5. Kroto, H. (1997) Symmetry, space, stars, and C_{60}. *Rev. Mod. Phys.*, 69: 703–722.
6. Smalley, R.E. (1997) Discovering the fullerenes. *Rev. Mod. Phys.*, 69: 723–730.
7. Schmalz, T.G., Seitz, W.A., Klein, D.J., and Hite, G.E. (1986) C_{60} carbon cages. *Chem. Phys. Lett.*, 130: 203–207.
8. Kroto, H.W. (1987) The stability of the fullerenes C_n, with n = 24, 28, 32, 36, 50, 70, and 70. *Nature*, 329: 529–531.
9. Bourgeois, L.N. and Bursill, L.A. (1997) High-resolution transmission electron microscopy and energetics of flattened carbon nanoshells. *Chem. Phys. Lett.*, 277: 571–578.

10. Kuznetsov, V.L., Chuvilin, A.L., Butenko, Y.V., Stankus, S.V., Khairulin, R.A., and Gutakovskii, A.K. (1998) Closed curved graphite-like structures formation on micron-size diamond. *Chem. Phys. Lett.*, 289: 353–360.

11. Boorum, M.M., Vasil'ev, Y.V., Drewello, T., and Scott, L.T. (2001) Groundwork for a rational synthesis of C_{60}: cyclodehydrogenation of a $C_{60}H_{30}$ polyarene. *Science*, 294: 828–831.

12. Tarasov, B.P., Goldshleger, N.F., and Moravsky, A.P. (2001) Hydrogen-containing carbon nanostructures: synthesis and properties. *Russ. Chem. Rev.*, 70: 131–146.

13. Fowler, P.W., Heine, T., and Troisi, A. (1999) Valencies of a smaller fullerene: structure and energetics of $C_{24}H_{2m}$. *Chem. Phys. Lett.*, 312: 77–84.

14. Zhu, H.Y. and Klein, D.J. (1995) Tetrahedral symmetry tetrahydrofullerenes. *J. Mol. Struct. Theochem*, 338: 11–23.

15. Klein, D.J. and Zhu, H.-Y. (1997) All-conjugated carbon species. In *From Chemical Topology to Three-Dimensional Geometry*; Balaban, A.T., Ed.; Plenum Press: New York, 297–342.

16. Balaban, A.T. and Harary, F. (1968) Chemical graphs. V. Enumeration and proposed nomenclature of benzenoid *cata*-condensed polycyclic aromatic hydrocarbons. *Tetrahedron*, 24: 2505–2516.

17. Liu, X., Klein, D.J., and Schmalz, T.G. (1994) Preferable fullerenes and Clar sextet cages. *Fuller. Sci. Technol.*, 2: 405–422.

18. Cataldo, F. (2003) Fullerane, the hydrogenated C_{60} fullerene: properties and astrochemical considerations. *Fullerenes, Nanotubes, and Carbon Nanostructures*, 11: 295–316.

19. Boltalina, O.V., Markov, V.Y., Troshin, P.A., Darwish, A.D., Street, J.M., and Taylor, R. (2001) $C_{60}F_{20}$: "Saturnene", an extraordinary squashed fullerene. *Angew. Chem. Int. Ed.*, 40: 787–789.

20. Boltalina, O.V., Markov, V.Y., Taylor, R., and Waugh, M.P. (1996) Preparation and characterization of $C_{60}F_{18}$. *Chem. Commun.*, 2549–2550.

21. Meier, M.S., Weedon, B.R., and Spielmann, H.P. (1996) Synthesis and isolation of one isomer of $C_{60}H_6$. *J. Am. Chem. Soc.*, 118: 11682–11683.

22. Clare, B.W. and Kepert, D.L. (2003) Structures, stabilities and isomerism in $C_{60}H_n$, $n = 2–36$. A comparison of the AM1 Hamiltonian and density functional techniques. *J. Mol. Struct. (Theochem)*, 622: 185–202.

23. Clare, B.W. and Kepert, D.L. (1997) Stereochemical patterns in $C_{60}X_n$. *J. Phys. Chem. Solids*, 58: 1815–1821.

24. Birkett, P.R., Avent, A.G., Darwish, A.D., Kroto, H.W., Taylor, R., and Walton, D.R.M. (1995) Formation and characterization of $C_{70}Cl_{10}$. *Chem. Commun.*, 683–684.

25. Huang, R., Xie, S., Tang, Z., Wang, Y., Huang, W., Chen, H., and Zheng, L. (1999) Studies of the formation of carbon clusters. *J. Cluster Sci.*, 10: 383–396.

26. Xie, S., Gao, F., Lu, X., Huang, R., Wang, C., Zhang, X., Liu, M., Deng, S., and Zheng, L. (2004) Capturing the labile fullerene[50] as $C_{50}Cl_{10}$. *Science*, 304: 699.

27. Bailey, S.W.D. and Lambert, C.J. (2004) Ab initio results for the electronic structure of $C_{50}Cl_{10}$, Los Alamos Natl. Lab., Preprint archive. *Condensed Matter*, 1–2.

28. Xie, R., Bryant, G.W., Cheung, C.F., Smith, V.H., Jr, and Zhao, J. (2004) Optical excitation and absorption spectra of $C_{50}Cl_{10}$. *J. Chem. Phys.*, 121: 2849–2851.

29. Okotrub, A.V. and Bulusheva, L.G. (1998) CKα-Spectra and investigation of electronic structure of fullerene compounds. *Fuller. Sci. Technol.*, 6: 405–432.

30. Babić, D., Došlić, T., Klein, D.J., and Misra, A. (2004) Kekulénoid addition patterns for fullerenes and some lower homologs. *Bull. Chem. Soc. Jpn.*, 77: 1–8.
31. Bulusheva, L.G., Okotrub, A.V., and Yudanov, N.F. (1997) Investigation of the electronic structure of $C_{60}F_{24}$. *J. Phys. Chem.*, 101: 10018–10028.
32. Limonov, M.F., Kitaev, Y.E., Chugreev, A.V., Smirnov, V.P., Grushko, Y.S., Kolesnik, S.G., and Kolesnik, S.N. (1998) Phonons and electron-phonon interaction in halogen-fullerene compounds. *Phys. Rev. B*, 57: 7586–7594.
33. Matsuzawa, N., Fukunaga, T., and Dixon, D.A. (1992) Electronic structures of 1,2- and 1,4-$C_{60}X_{2n}$ derivatives with $n = 1, 2, 4, 6, 8, 10, 12, 18, 24$, and 30. *J. Phys. Chem.*, 96: 10747–10756.
34. Denisenko, N.I., Troyanov, S.I., Popov, A.A., Kuvychko, I.V., Zemva, B., Kemnitz, E., Strauss, S.H., and Boltalina, O.V. (2004) T_h-$C_{60}F_{24}$. *J. Am. Chem. Soc.*, 126: 1618–1619.